A small-angle X-ray scattering study of the effect of chain architecture on the shear-induced crystallization of branched and linear poly(ethylene terephthalate)

Tracey Hanley,[a]* David Sutton,[a]‡ Ellen Heeley,[b]¶ Graeme Moad[c] and Robert Knott[a]

[a]ANSTO, Private Mail Bag, Menai, NSW 2234, Australia, [b]Department of Chemistry, The University of Sheffield, Western Bank, Sheffield S10 2TN, United Kingdom, and [c]CSIRO Molecular and Health Technologies, Bag 10, Clayton South VIC 3169, Australia. Correspondence e-mail: tracey.hanley@ansto.gov.au

The synchrotron-based small-angle X-ray scattering (SAXS) technique was used to investigate the shear-induced crystallization kinetics of branched/unbranched poly(ethylene terephthalate) (PET). Reactive extrusion of bottle-grade PET with the branching and chain-extension agents pyromellitic dianhydride and pentaerythritol results in enhanced rheological properties, such as higher melt strength and higher viscosity. In this study, six samples of PET were investigated: linear PET [intrinsic viscosity (IV) $\simeq$ 0.76 dm^3 g^{-1}]; four branched PETs produced from linear PET by a reactive extrusion technique (IV $\simeq$ 0.86–1.06 dm^3 g^{-1}); and a control PET (IV $\simeq$ 0.73 dm^3 g^{-1}) extruded under the same conditions without reactive agents. SAXS data were recorded for the PET at the melt temperature and time-resolved SAXS data were recorded following the application of a step shear (53 s^{-1} for 2 s). As the PET IV was increased, the extent of shear-induced orientation increased, whilst the time taken for the polymer to initiate and complete crystallization decreased.

1. Introduction

The majority of commercial polymer processing involves the application of shear stresses to molten polymers. To analyse the effects of polymer architecture combined with shear stress, a study was undertaken on the crystallization kinetics of a series of different grades of poly(ethylene terephthalate) (PET) prepared using a novel reactive extrusion process (Van Diepen *et al.*, 1998). Reactive extrusion of bottle-grade PET with the branching and chain-extension agents pyromellitic dianhydride (PMDA) and pentaerythritol (penta) resulted in enhanced rheological properties, such as higher melt strength and higher viscosity (Van Diepen *et al.*, 1998; Forsythe *et al.*, 2006).

A key finding of a previous isothermal crystallization study of these novel PETs under quiescent conditions (zero shear) (Hanley *et al.*, 2006) was that the reactive extrusion process significantly modified the crystallization kinetics and changed the final polymer morphology. In summary, the rate of melt crystallization of the branched PET was reduced by up to ~20% and the lamella spacing reduced by ~10%. In particular it was found that varying the relative amounts of PMDA and penta gave significantly higher melt strengths and viscosities compared to the addition of PMDA alone. The improvements as a result of co-addition included lower extruder torque values, die pressures and melt temperatures, and consequently lower levels of degradation. The additives worked in two ways: (i) the alcoholysis of the PET by the added penta produced a branched PET; and (ii) the PMDA caused chain extension and repair of the chain scissions that occur during alcoholysis. The resulting PET was

investigated by a combination of rheology, end-group analyses and gel permeation chromatography (GPC) and was found to be a hyperbranched polyester with long-chain branching (Forsythe *et al.*, 2006). The extent of branching and the length of branches were related to the concentrations of co-additives used in the reactive extrusion process.

Small-angle X-ray scattering (SAXS) is a valuable technique for exploring the crystallization kinetics of polymers. SAXS investigations of PET crystallization have been the subject of many previous studies (Haubruge *et al.*, 2004, 2003; Xia *et al.*, 2001; Ivanov *et al.*, 2001; Wang *et al.*, 1999; Rule *et al.*, 1995; Lee *et al.*, 2003; Mahendrasingam *et al.*, 2003; Sutton *et al.*, 2005); however, none to date have focused on branched PET, apart from our own quiescent studies (Hanley *et al.*, 2006). In an attempt to more closely approximate commercial processing conditions, several research groups are currently conducting real-time SAXS experiments to study shear-induced crystallization, especially in thermoplastics (Heeley *et al.*, 2003; Koscher & Fulchiron, 2002; Agarwal *et al.*, 2003; Stribeck *et al.*, 2004; Somani *et al.*, 2000; Kornfield *et al.*, 2002; Kumaraswamy *et al.*, 2004; Duplay *et al.*, 2000). The present study followed this trend, where model shear experiments were combined with *in-situ* SAXS measurements. These dynamic measurements allow the effects of chain architecture to be investigated during the molecular structure development stage.

The shear-induced crystallization of polymers has been found previously to depend upon the molar mass components of the polymer material as well as the type and extent of branching. Seki *et al.* (2002) were able to demonstrate the key role played by a small percentage of the high molar mass component in polypropylene (PP) in shear-induced crystallization. It was found that above a critical

‡ Present address: MDL Basell, Geelong, Australia
¶ Present address: Chemistry Department, The Open University, UK

Table 1
PET sample compositions and comparison of GPC data with IV and MFI.

	Reactive extrusion additives		GPC results†					IV (dm^3 g^{-1}) ($\pm$ 0.01)	MFI [g (10 min)$^{-1}$]
Sample	PMDA‡	penta§	M_n	M_w	M_z	M_p	M_w/M_n		
V	No reactive extrusion		–	–	–	–	–	0.76	23.6
A	None	None	21930	61080	94150	71810	2.79	0.73	36.2
B	0.15	None	22890	81670	151400	76030	3.57	0.87	13.3
C	0.15	5:1	23760	77590	145000	74990	3.27	0.86	–
D	0.35	5:1	21440	94590	235400	73390	4.41	1.02	–
E	0.4	5:1	21690	97120	243200	74990	4.48	1.06	9.9

‡ wt% of PMDA added in the reactive extrusion process. § Molar ratio of PMDA:pentaerythritol. † PET-B, C, D and E are branched polymers therefore GPC results are underestimated. M_n is number average molecular weight, M_w is weight average molecular weight, M_z is z-average molecular weight, and M_p is peak average molecular weight.

concentration, the rate of crystallization was increased and the degree of orientation in the final morphology was also increased. It was suggested that the high molar mass components had more entanglements and therefore a greater extent of chain alignment that had a nucleating effect on the subsequent crystallization process. In a further study by Agarwal *et al.* (2003) on the effect of long-chain branching of isotactic PP (iPP), it was found that the shear-induced crystallization was significantly altered to that of linear iPP. Long-chain branching increased the amount of induced orientation as well as increasing the rate of crystallization, which was attributed to the long relaxation time of the highly branched species acting as nucleating sites.

It was intended in this study to observe the effect of chain architecture on the shear-induced crystallization of novel PETs. The synchrotron-based SAXS technique was used to investigate the shear-induced crystallization kinetics of branched/unbranched PETs. Six types of PET were investigated: linear (unprocessed) PET; four branched PETs produced from linear PET by a reactive extrusion technique; and a control PET extruded under the same conditions without reactive agents.

2. Experimental

In this study, the six PETs were chosen to cover a wide range of the possible sample preparation variables, and thus the end products. Table 1 is a summary of the sample properties, which include the reactive extrusion additive concentrations, chromatography results (GPC), intrinsic viscosity (IV), and melt flow indices (MFIs). PET-V was a commercially available PET, Eastman PET 9663 E0002, purchased from Eastman Chemical Company and used as received. PET-A was a control sample prepared by processing PET-V in the extruder under the same conditions as used for the reactive extrusion, but without any chemical additives. This process gives a direct measure of the degree of degradation and change that occurred as a result of the heating and shearing processes. The other four samples (PET-B, C, D and E) were prepared by reactive extrusion of the PET-V with chemical additives; a tetrafunctional acid anhydride pyromellitic dianhydride (PMDA) (supplied by Indspec, USA) and a polyhydric alcohol pentaerythritol, added in different concentrations for the different samples. The reactive extrusion was performed using a JSW TEX-30 twin screw extruder in a co-rotating mode at 553 K.

IV measurements were measured in duplicate using a PAAR AMW200 viscometer at 303 K. PET samples of 0.1 g were dissolved in 25 ml of solvent (60/40 w/w phenol/tetrachloroethane mixture) at 378 $\pm$ 2 K for 30 min prior to measurement.

GPC was performed on a Hewlett Packard 1090 liquid chromatograph equipped with a diode array detector. The detection wavelength was 270 nm. A set of four Waters Styrogel columns (HR1, HR2, HR4, HT5 each 7.8 $\times$ 300 mm) were used which covered the nominal molecular weight (M_w) range 200–10^6 g mol^{-1}. The eluting solvent was 0.01 M tetrabutyl ammonium acetate in chloroform:hexafluoroisopropanol (HFIP) (9:1 v/v) at 1 ml min^{-1}. The GPC columns were calibrated with broad PET standards (American Polymer Standards, USA). Samples were prepared by first dissolving the PET in a 50:50 v/v chloroform:HFIP solution and diluting this with the appropriate volume of chloroform to attain a 9:1 v/v chloroform:HFIP ratio and a PET concentration of approximately 1 mg ml^{-1}. It has been shown that quantification and direct comparisons of the M_w of the branched PET with its linear precursors cannot be made by GPC, since the hydrodynamic volume of the branched polymers is less than that of linear polymers with similar M_ws. Therefore the observed GPC M_w for branched polymers will be an underestimate of (i) the actual M_w, and (ii) the width of the M_w distribution.

The MFI was measured with a Tinius Olsen Plastometer according to ASTM D1238 at 558 K with a load of 2.1 kg.

SAXS data were obtained on the DUBBLE beamline (BM26) at the European Synchrotron Radiation Facility (Grenoble, France) (Borsboom *et al.*, 1998). An X-ray beam with a wavelength (λ) of 1.24 Å (10 keV) was used and a sample-to-detector distance of 2.5 m was selected providing a total scattering vector range of 0.01 < q < 0.13 Å^{-1} ($q = 4\pi \sin \theta / \lambda$, where θ is half the Bragg scattering angle 2θ). The Linkam CSS-450 shear cell (Linkam UK) was modified to be purged with dry nitrogen gas for all experiments to minimize hydrolysis of PET at elevated temperatures. A silver behenate standard was placed inside the shear cell to calibrate the scattering angle. The temperature of the polymer samples inside the shear cell was calibrated using a thermocouple placed within the molten polymer. Samples were dried in a vacuum oven at 398 K for 8 h prior to SAXS measurements. Samples were placed in the shear cell between stainless steel plates fitted with mica windows with a distance of 500 $\pm$ 10 µm between the plates. All experiments were conducted according to the following protocol: samples were first melted at 573 K for 5 min to remove previous thermal history, and then cooled at 30 K min^{-1} to 553 K where a step shear was applied for 2 s at a shear rate of 53 s^{-1}. Finally, samples were immediately cooled at 30 K min^{-1} to the crystallization temperature of 518 K where isothermal crystallization proceeded. SAXS data were recorded for the molten polymers at the melt temperature and time-resolved SAXS data were recorded following the application of the step shear. The data analysis and display package *Fit2D* was used extensively (Hammersley, 1998).

3. Results and discussion

Zero-shear isothermal crystallization of PET-A, B, C, D, E and V after heating to 573 K for melting and then quenching to 518 K proceeded
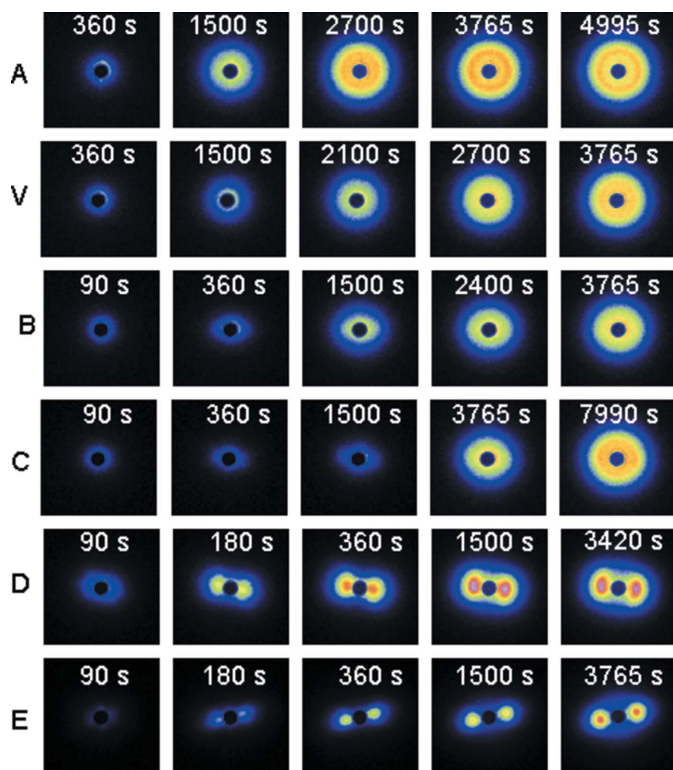
Figure 1
Two-dimensional SAXS patterns (scattering vector range: $0 < q < 0.13$ Å^{-1}) of the six different PET samples studied for shear-induced crystallization (time after step shear given for each frame).

too slowly to be observed in this series of experiments, with crystallization times in excess of several hours required (results not shown).

The SAXS two-dimensional images for PET-A, B, C, D, E and V at particular times after the step shear are shown in Fig. 1. PET-A and V show isotropic crystallization behaviour (Fig. 2) with the application of shear required to initiate crystallization as expected and a rate of crystallization considerably faster than the observed zero-shear isothermal crystallization at these temperatures. PET-A crystallized faster than PET-V, which is a molecular weight effect and due to both the smaller overall M_w of the PET chains and the broader M_w distribution of the PET-A. During processing the polymer chains undergo chain scission reactions resulting in a lower overall M_w as well as a large increase in the small-chain components. These components can fold and rearrange on a faster timescale, as well as participate in secondary crystallization more easily than long-chain molecules, being able to fold in a confined space either between existing spherulites or interstitially between branch arms. Conversely, the longer chains of PET-V restricted the ability of the polymer to crystallize. At these temperatures there was sufficient molecular motion to allow time for relaxation of the initial shear-induced orientation leading to isotropic crystallization (Fig. 2).

PET-B, C, D and E have higher IVs, greater M_ws as revealed by GPC, and lower MFIs indicating significant increase in the M_w of the polymer chains as well as increased branching. PET-B and PET-C behaved similarly to one another but differently to the other PETs, showing shear-oriented crystallization at the beginning of the crystallization and finishing with almost isotropic scattering patterns (Figs. 2 and 4). Compared to both PET-A and V, the crystallization initiation occurred more quickly but overall crystallization at longer times proceeded more slowly than the linear counterparts shown in Fig. 3. Both PET-B and C followed the same crystallization pathways

shown by the shape of the curves in Fig. 3. Faster initiation of crystallization is unexpected from the increased M_w of PET-B and C, leading to faster nucleation of the string nuclei and therefore a greater number of nucleation points within the samples. The balance between the rate of crystallization and the molecular motion at the crystallization temperatures allows sufficient relaxation for the samples to form almost isotropic scattering. The IVs of PET-B and C are very similar, although the GPC data suggest that PET-C is lower in M_w than PET-B. The most likely scenario is that PET-C is slightly more branched than PET-B and therefore the overall M_w of PET-C is higher than that of PET-B.

Incarnato *et al.* (2000) found that the introduction of PMDA alone by reactive extrusion introduced long-chain branching and broadening of the M_w distribution. In a study by Forsythe *et al.* (2006) on the rheological properties of reactively extruded PET, it was found that the dominant process by addition of PMDA was chain extension with minimal branching. It was shown that when penta was used in conjunction with PMDA in the appropriate ratio, the introduction of penta was responsible for the introduction of branch points. Therefore in PET-B the introduction of branching was observed but chain extension dominated, whereas PET-C has a higher number of branch points from added penta but crystallized more slowly, which is expected from the increase in M_w. The characteristic shape of the scattering intensity *versus* time curves for both PET-B and C (Fig. 3) shows that the shear initiated a rapid oriented crystallization followed by slower isotropic crystallization, which indicates both samples have branch points acting as nucleating sites. At low concentrations of PMDA and penta, Forsythe *et al.* (2006) found that the major process was still chain extension rather than branching, so PET-B and C are most likely to have low numbers of branch points. The IVs of PET-B and C are very similar, and although the GPC analysis showed the M_w of PET-C to be lower, the crystallization kinetics implies that M_w is higher. This can easily be explained by the fact that PET-C has a higher number of long-chain branch points than PET-B. The orientation function shown in Fig. 4 shows that both PET-B and C initially crystallized with a high degree of orientation (*i.e.* low orientation function) then as time progressed the samples became less oriented
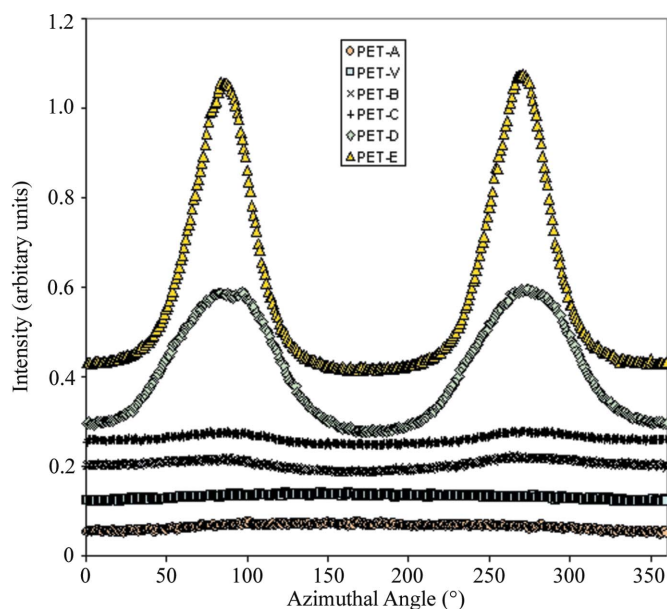

Figure 2
Variation of scattering intensity with azimuthal angle for the final frames of each PET. Note: the plots have been offset for clarity with PET-A at the bottom and PET-E at the top.

approaching an isotropic value of 1.0. It is also seen in Fig. 2 that the degree of orientation change with azimuthal angle is almost constant, although a slight preferred orientation is still observable under these experimental conditions.

PET-D and E have the highest concentration of additives and showed the fastest crystallization as well as the highest degree of orientation. The high number of long-chain branch points provides a very large number of shear-induced nucleation points. Crystallization was accelerated to the point where, even at the high crystallization temperature used in this study, the crystallization occurred too rapidly to allow any relaxation of the polymer chains. The most branched and highest M_w sample, PET-E, exhibited the highest degree of orientation. Comparisons of the overall orientation achieved by each sample at the end of the crystallization period are shown by the scattering intensity *versus* azimuthal angle plots in Fig. 2. The orientation functions of PET-D and E (Fig. 4) initially (*i.e.* time ≤ 70 s) show an increase (number greater than 1.0) followed by a rapid decrease to a very low value that is reasonably constant with time, indicating the development of the lamellae in a highly oriented fashion. The initial increase in orientation function is due to the equatorial streaking indicative of shish formation (Agarwal *et al.*, 2003) which dominates the scattering at the very early stages of crystallization; this is very quickly exceeded by the scattering from the crystallization of lamellae perpendicular to the shear direction.

The increased concentrations of additives in the reactive extrusion process (i) produce a larger number of branch points and (ii) cause increased chain extension to occur (Hanley *et al.*, 2006; Forsythe *et al.*, 2006). The higher number of branch points and chain extension is shown most clearly by the increase in IV. The trend of the observed SAXS results was faster initiation of crystallization with increased IV and more orientation in the final morphologies. These results show that a higher M_w for PET-D and E clearly leads to a longer relaxation time after the step shear due to an increased level of entanglements between the polymer chains. Other research groups using polyolefins have shown that high M_w chains, when oriented in this way, can have a nucleating effect for the crystallization that follows resulting in enhanced crystallization kinetics (Seki *et al.*, 2002).

Previous studies of the branching of PET have shown branching to affect the crystallization kinetics resulting in both more rapid crystallization and slower crystallization (Bikiaris & Karayannidis, 2003; Jayakannan & Ramakrishnan, 1999; Kint & Munoz-Guerra, 2003; Rosu *et al.*, 1997; Rosu *et al.*, 1999; Scheirs & Long, 2003). It seems that knowledge of branching alone is not sufficient to predict the crystallization kinetics. Introduction of branching can slow kinetics, but with an increased number of branch points and an increase in the length of branches the kinetics become increasingly more rapid. The degree of shear-induced orientation was, on the other hand, found to be directly proportional to the IV. An increase in IV led to an increase in the degree of orientation. It was also shown that in both linear PET-A and V, and branched PET-B and C, an increase in M_w lead to slower crystallization rates, but in the long-chain branched PET-D and E an increase in M_w increased the rate of crystallization. This suggests that there is a threshold which introduces a change in the underlying mechanism of the crystallization, most likely attributed to the number of branches as well as the length of the branches themselves.

The crystallization of the various PET samples was strongly dependent on the PET properties. The highly branched, high M_w PET-D and E have a very large degree of orientation induced by the shear event, whereas the linear PET-A and V had isotropic crystallization induced by the step shear (*i.e.* they crystallize more rapidly than if allowed to crystallize isothermally without shear). In contrast,
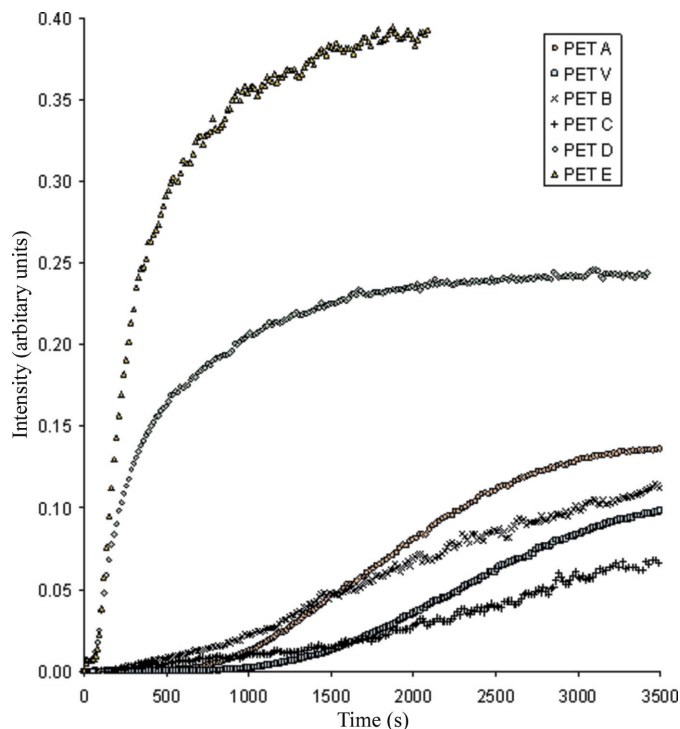

Figure 3
Total integrated scattering intensity as a function of time following the step shear.

the two intermediate PETs, PET-B and C, had orientation-induced crystallization initially followed by isotropic crystallization.

PET-V was the starting linear polymer with a low M_w distribution. The processed version of PET-V therefore was also a linear polymer with lower M_w and broader M_w distribution. PET-B contained PMDA alone and with a small number of branch points *but* predominantly increased chain length. PET-C had lower chain length than PET-B, a similar concentration of branch points but longer branches than PET-
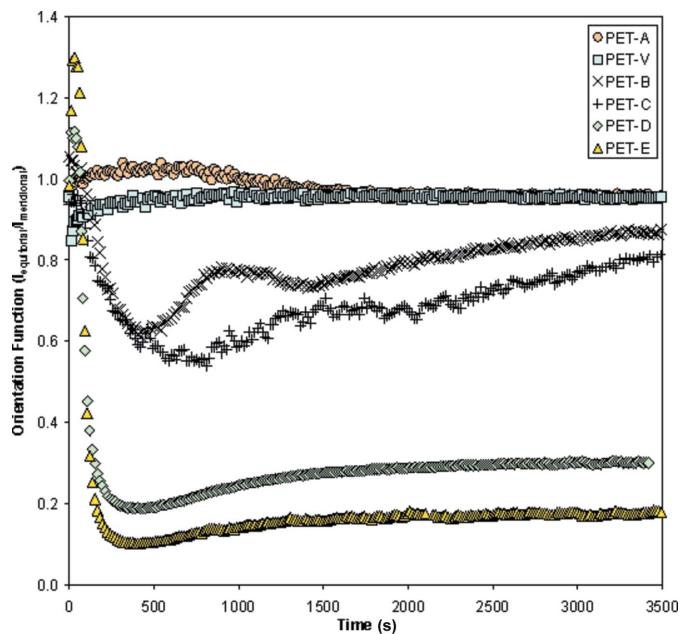

Figure 4
Change in orientation function with time following the step shear for the six PETs. The orientation function is defined as the integrated intensity in the equatorial direction divided by the integrated intensity in the meridional direction.

B, and hence the overall M_w was similar for PET-B and C. Introduction of both PMDA and penta gave hyperbranched structures. PET-D and E are hyperbranched long-chain molecules with increased number of branches with increasing PMDA and penta.

Overall it was found that the branch points acted as nucleation sites with initiation of crystallization faster in all the branched materials. However, with low numbers of branch points, the rate of crystallization proceeded slower, in contrast to long-chain hyperbranched PET samples where both initiation and progression of crystallization were very rapid. This can be explained by the branch points acting as nucleating sites, but then at low numbers of branch points the crystallization proceeded at a rate that allowed relaxation of the chains *i.e.* the observation that the crystallization then became isotropic and the chain folding required for crystallization was inhibited by the chain entanglements that have occurred as a result of the initial shear-induced crystallization. Conversely, the hyperbranched molecules with long-chain branching crystallized so rapidly upon the application of shear that there is very little time for relaxation, as evidenced by the degree of shear-induced orientation.

What has been observed was that the introduction of branch points promoted crystallization and while in the linear chains the crystallization was more rapid than without the step shear, it occurred isotropically. The long-chain hyperbranched PET-D and E crystallized very rapidly upon application of shear and substantial preferred orientation resulted. The two intermediate PETs, PET-B and C, are the most interesting where it was observed that two separate crystallization processes were occurring. The initial crystallization proceeded similarly to the more highly branched materials PET-D and E, while at longer times the crystallization proceeded more like the linear chain PETs PET-A and V. Conceptually, this phenomenon is due to the parts of the chain adjacent to the branch points crystallizing and forming relatively large crystallized objects. Then, the remainder of the polymer chain has to crystallize, but it is hindered by the already crystallized material. The chain-folding mechanism of the entangled and partially crystallized chains then slows the crystallization process significantly, although now the crystallization is occurring in an isotropic fashion with a more regular spherulitic growth pattern.

Polymer crystallization theory on the nucleation and growth mechanisms for PET (Kaji, 2002; Nishida *et al.*, 2004; Olmsted *et al.*, 1998) indicates that spinodal-assisted crystallization occurs through regions within the molten polymer where polymer chains with longer persistence lengths align to minimize excluded volume. These regions have higher density that causes a bimodal liquid–liquid transition driven by chain conformation and regional density variations that give rise to spinodal-assisted crystallization. In a previous study on quiescent crystallization (Hanley *et al.*, 2006), it was suggested that long-chain hyperbranched polyesters promoted crystallization by one of three possibilities: (i) branch points acting as nucleating agents; (ii) long-chain branching assisting crystallization by increasing spinodal separation in the melt; or (iii) lower M_w fractions produced by the reactive extrusion process shortening the half-time of crystallization. The behaviour of PET-B and C indicates that (iii) can now be discounted as a potential mechanism as the overall crystallization half-time for these samples was actually increased, while (i) and (ii) remain valid. In the case of long-chain branching, the branch points would provide easy alignment points for more than one chain to align and therefore increase the conformational density variations and hence increase the potential for spinodal-assisted crystallization. The application of shear would increase the likelihood of chain alignments in this case and therefore result in lower induction times and more rapid crystallization.

4. Conclusion

Reactive extrusion of PET increased melt viscosity and had a large influence on the shear-induced crystallization. The presence of long-chain hyperbranched structures in the PET had a substantial impact on zero-shear isothermal crystallization (Hanley *et al.*, 2006), and this effect was accelerated under shear. The degree of orientation induced by the step shear was directly related to increased intrinsic viscosity of the material. The kinetics observed in this study and the degree of orientation achieved were strongly dependent on the type of PET used. Linear PET-A and V exhibited shear-induced isotropic crystallization that was slower with increasing M_w, while the reactive extruded long-chain branched PET-D and E showed the opposite trend, where increasing the M_w increased both the rate of crystallization and the degree of induced orientation of the final product. The intermediate PETs, PET-B and C, which have increased melt viscosity in comparison to linear PET-A and V, have increased kinetics and orientation initially but then proceed at a slower rate than the linear PET. In summary, the findings from this study establish that crystallization behaviours are critically dependent on the PET molecular architecture. Consequently, the commercial processing conditions for branched PET should be significantly different to those required for conventional linear PET. Conversely, branched PET would be capable of different processing regimes to those accessible by standard linear PET grades.

References

Agarwal, P. K., Somani, R. H., Weng, W., Mehta, A., Yang, L., Ran, S., Liu, L. & Hsiao, B. S. (2003). *Macromolecules*, **36**, 5226–5235.
Bikiaris, D. N. & Karayannidis, G. P. (2003). *Polym. Int.* **52**, 1230–1239.
Borsboom, M., Bras, W., Cerjak, I., Detollenaere, D., Glastra van Loon, D., Goedtkindt, P., Konijnenburg, M., Lassing, P., Levine, Y. K., Munneke, B., Oversluizen, M., van Tol, R. & Vlieg, E. (1998). *J. Synchrotron Rad.* **5**, 518–520.
Duplay, C., Monasse, B., Haudin, J. M. & Costa, J. L. (2000). *J. Mater. Sci.* **35**, 6093–6103.
Forsythe, J. S., Cheah, K., Nisbet, D. R., Gupta, R. K., Lau, A., Donovan, R., O'Shea, M. & Moad, G. (2006). *J. Appl. Polym. Sci.* **100**, 3646–3652.
Hammersley, A. P. (1998). ESRF Internal Report ESRF98HA01T, *FIT2D V9.129 Reference Manual* Version 3.1. Grenoble, France.
Hanley, T. L., Forsythe, J. S., Sutton, D., Moad, G., Burford, R. P. & Knott, R. B. (2006). *Polym. Int.* **55**, 1435–1443.
Haubruge, H. G., Gallez, X. A., Nysten, B. & Jonas, A. M. (2003). *J. Appl. Cryst.* **36**, 1019–1025.
Haubruge, H. G., Jonas, A. M. & Legras, R. (2004). *Macromolecules*, **37**, 126–134.
Heeley, E. L., Maidens, A. V., Olmsted, P. D., Bras, W., Dolbnya, I. P., Fairclough, J. P. A., Terrill, N. J. & Ryan, A. J. (2003). *Macromolecules*, **36**, 3656–3665.
Incarnato, L., Scarfato, P., Di Maio, L. & Acierno, D. (2000). *Polymer*, **41**, 6825–6831.
Ivanov, D. A., Amalou, Z. & Magonov, S. N. (2001). *Macromolecules*, **34**, 8944–8952.
Jayakannan, M. & Ramakrishnan, S. (1999). *J. Appl. Polym. Sci.* **74**, 59–66.
Kaji, K. (2002). *Handbook of Thermoplastic Polyesters*, edited by S. Fakirov, pp. 225–251. Weinheim: Wiley-VCH.

conference papers

Kint, D. P. R. & Munoz-Guerra, S. (2003). *Polym. Int.* **52**, 321–336.

Kornfield, J. A., Kumaraswamy, G. & Issaian, A. M. (2002). *Indust. Eng. Chem. Res.* **41**, 6383–6392.

Koscher, E. & Fulchiron, R. (2002). *Polymer*, **43**, 6931–6942.

Kumaraswamy, G., Verma, R. K., Kornfield, J. A., Yeh, F. & Hsiao, B. S. (2004). *Macromolecules*, **37**, 9005–9017.

Lee, B., Shin, T. J., Lee, S. W., Yoon, J., Kim, J., Youn, H. S. & Ree, M. (2003). *Polymer*, **44**, 2509–2518.

Mahendrasingam, A., Blundell, D. J., Wright, A. K., Urban, V., Narayanan, T. & Fuller, W. (2003). *Polymer*, **44**, 5915–5925.

Nishida, K., Kaji, K., Kanaya, T., Matsuba, G. & Konishi, T. (2004). *J. Polym. Sci. B Polym. Phys.* **42**, 1817–1822.

Olmsted, P. D., Poon, W. C. K., McLeish, T. C. B., Terrill, N. J. & Ryan, A. J. (1998). *Phys. Rev. Lett.* **81**, 373–376.

Rosu, R. F., Shanks, R. A. & Bhattacharya, S. N. (1997). *Polym. Int.* **42**, 267–275.

Rosu, R. F., Shanks, R. A. & Bhattacharya, S. N. (1999). *Polymer*, **40**, 5891–5898.

Rule, R. J., MacKerron, D. H., Mahendrasingam, A., Martin, C. & Nye, T. M. W. (1995). *Macromolecules*, **28**, 8517–8522.

Scheirs, J. & Long, T. E. (2003). *Modern Polyesters: Chemistry and Technology of Polyesters and Copolyesters*. New York: John Wiley.

Seki, M., Thurman, D. W., Oberhauser, J. P. & Kornfield, J. A. (2002). *Macromolecules*, **35**, 2583–2594.

Somani, R. H., Hsiao, B. S., Nogales, A., Srinivas, S., Tsou, A. H., Sics, I., Balta-Calleja, F. J. & Ezquerra, T. A. (2000). *Macromolecules*, **33**, 9385–9394.

Stribeck, N., Camarillo, A. A., Cunis, S., Bayer, R. K. & Gehrke, R. (2004). *Macromol. Chem. Phys.* **205**, 1445–1454.

Sutton, D., Wanrooij, P., Hanley, T., Burford, R. P., Heeley, E. & Knott, R. B. (2005). *J. Macromol. Sci. Phys.* **44**, 1–19.

Van Diepen, G., O'Shea, M. & Moad, G. (1998). *Modified polyesters*. World Patent WO 98/33837.

Wang, Z.-G., Hsiao, B. S., Fu, B. X., Liu, L., Yeh, F., Sauer, B. B., Chang, H. & Schultz, J. M. (1999). *Polymer*, **41**, 1791–1797.

Xia, Z., Sue, H.-J., Wang, Z., Avila-Orta, C. A. & Hsiao, B. S. (2001). *J. Macromol. Sci. Phys.* **B40**, 625–638.